

Temperature and Strain Coefficient of Velocity for Langasite SAW Devices

W. C. Wilson*, G. M. Atkinson**

*NASA Langley Research Center, Hampton, VA, USA, w.c.wilson@larc.nasa.gov

**Virginia Commonwealth University, Richmond, VA, USA, gmatkins@vcu.edu

ABSTRACT

Surface Acoustic Wave sensors on Langasite substrates are being investigated for aerospace applications. Characterization of the Langasite material properties must be performed before sensors can be installed in research vehicles. The coefficients of velocity for both strain and temperature have been determined. These values have also been used to perform temperature compensation of the strain measurements.

Keywords: Surface Acoustic Wave, SAW, strain, temperature, Langasite, coefficient of velocity.

1 INTRODUCTION

Surface Acoustic Wave (SAW) strain gauges made with new materials such as Langasite are being investigated by NASA's Vehicle Systems Safety Technologies (VSST) project for aviation safety applications. Strain gages have been used for structural health monitoring applications such as monitoring load conditions, fatigue, and to detect cracks in airframes [1]. SAW strain sensors can provide more information while adding negligible weight. SAW devices have been demonstrated in environments from cryogenic to high temperatures and are immune to vibration, radiation, and pressure changes [2]. In order to develop sensors that can operate in the harsh environments found in aerospace vehicles, these new materials must be fully characterized. The coefficients of velocity for both strain and temperature must be determined so that accurate measurements during aircraft flight conditions can be achieved.

2 BACKGROUND

Strain is defined as the change in length of an object, divided by the original length; therefore strain (ϵ) is given by:

$$\epsilon = \frac{\Delta L_S}{L}, \quad (1)$$

where ΔL_S is the change in length due to strain and L is the original length of the device. For repeatable measurements the SAW devices must operate inside of the elastic portion of the stress-strain curve for the material. Stretching and compressing the device will cause the finger widths and spaces to change, and will therefore change the wavelength (λ) of a SAW device. Changes in wavelength will cause a

change in the frequency of operation of the SAW device. The synchronous or center frequency (f) of a SAW device is related to the velocity of the acoustic wave (v) and the wavelength (λ) and is given by:

$$f = \frac{v}{\lambda}. \quad (2)$$

In addition to the wavelength, strain will also cause the elastic coefficients and the density to change [3]. Both of these parameters affect the acoustic wave propagation and are manifested in changes in the velocity (v) of the SAW device. Since both the velocity and wavelength affect the frequency, both will have to be considered when examining the changes due to strain. To do this, each of the changes is divided by its original value to yield a fractional value. The fractional change in frequency (Δf_S) due to the fractional change in the velocity (Δv_S) from strain, and the fractional change in length (ΔL_S) from strain is given by [4]:

$$\frac{\Delta f_S}{f} = \frac{\Delta v_S}{v} - \frac{\Delta L_S}{L} = \frac{\Delta v_S}{v} - \epsilon. \quad (3)$$

The strain coefficient (γ_S) of velocity for uniaxial strain is defined as [4]:

$$\frac{\Delta v}{v} = \gamma_S \epsilon. \quad (4)$$

The strain coefficient is highly dependent on the anisotropic material parameters, and therefore it is dependent on the crystallographic orientation of the substrate and the propagation direction on the substrate. The strain coefficient yields an equation that relates the fractional frequency to the strain [4] and is given by:

$$\frac{\Delta f_S}{f} = (\gamma_S - 1)\epsilon. \quad (5)$$

Like strain, temperature causes both a change in length of an object and material parameter changes such as density and elastic coefficients. The linear thermal coefficient of expansion is defined as the change in length divided by the original length caused by thermal expansion; therefore the linear thermal coefficient of expansion (α) is given by:

$$\alpha = \frac{\Delta L_T}{L_T}, \quad (6)$$

where ΔL_T is the change in length due to a temperature change and L_T is the original length of the device. Again, the stretching and compressing of the device will cause the finger widths and spaces to change, and will therefore change the wavelength (λ) of the device resulting in changes in the frequency of operation of the SAW device (Eqn. 2). Also, both the elastic coefficients and density changes will affect the velocity (v) of the SAW device. These changes lead to a fractional change in frequency due to the fractional change in the velocity and the fractional change in length due to temperature which is given by [5]:

$$\frac{\Delta f_T}{f} = \frac{\Delta v_T}{v} - \frac{\Delta L_T}{L_T} = \frac{\Delta v_T}{v} - (\alpha_1 \Delta T + \alpha_2 \Delta T^2). \quad (7)$$

There are two temperature coefficients in (7), the first order (α_1), and the second order (α_2) [6]. For a Languisite substrate the values of $\alpha_1 = 5.68$, and $\alpha_2 = 5.43$ will be used [7]. The temperature coefficient of velocity (γ_T) is defined as [5]:

$$\frac{\Delta v_T}{v} = \gamma_T \frac{\Delta L_T}{L} = \gamma_T (\alpha_1 \Delta T + \alpha_2 \Delta T^2). \quad (8)$$

Similar to the strain case, the temperature coefficient of velocity will yield an equation that relates the fractional frequency to the temperature and is given by:

$$\frac{\Delta f_T}{f} = (\gamma_T - 1)(\alpha_1 \Delta T + \alpha_2 \Delta T^2). \quad (9)$$

The combined effects from temperature and strain are found by combining equations (5) & (9) into a single equation given by:

$$\frac{\Delta f}{f} = (\gamma_S - 1)\varepsilon + (\gamma_T - 1)(\alpha_1 \Delta T + \alpha_2 \Delta T^2). \quad (10)$$

Rearranging (eqn. 10) yields the temperature compensated strain:

$$\varepsilon = \frac{\frac{\Delta f}{f} - (\gamma_T - 1)(\alpha_1 \Delta T + \alpha_2 \Delta T^2)}{(\gamma_S - 1)}. \quad (11)$$

3 EXPERIMENTAL SETUP

The SAW devices are fabricated on Languisite ($\text{La}_3\text{Ga}_5\text{SiO}_{14}$) (LGS) substrates. The sensor has four Orthogonal Frequency Coded (OFC) reflector banks which spread the device's response across multiple frequencies through the use of OFC reflectors [8]. The device has two identical tracks due to fabrication constraints, where each reflector bank is comprised of four gratings (Fig. 1.). The

gratings in each track reflect a different frequency and are arranged sequentially in ascending order as they are positioned further from the interdigitated transducer (IDT).

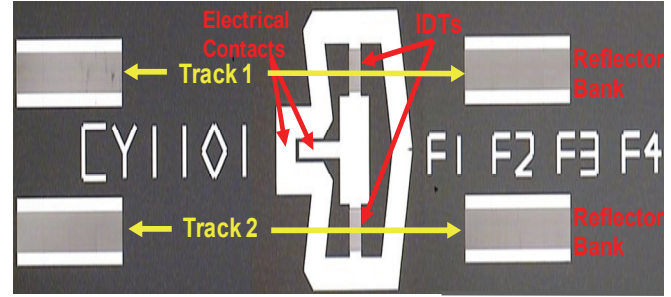


Fig. 1. SAW OFC strain sensor. The tracks are shown in yellow, the IDTs, reflector banks, and electrical contacts are all identified in red.

Expansion of the SAW device results in a decrease in the operating frequency, due to tensile strain or an increase in temperature, while contraction due to compressive strain or reduced temperature will result in an increase in the operating frequency. These changes are due in part to the change in the wavelength and a change in the average propagation velocity of the surface acoustic wave. The velocity changes are due to changes from the stiffness parameters and the density of the material [9].

For this investigation an OFC SAW strain sensor and a foil strain gauge were bonded onto a stainless steel bar. The bar is 304 stainless steel, 45.75 cm long, 5 cm wide and 0.635 cm thick. The conventional strain gauge is a general purpose 350 Ω foil strain gauge part number WK-13-125AD-350W from Vishay. A type K thermocouple was placed in contact with the bar between the SAW sensor and the strain gauge. The bar was configured for cantilever loading.

4 RESULTS

To characterize the strain response of the SAW sensor, multiple experiments were performed. For the first experiment the load was increased from 0 kg to 1.0 kg in 0.1 kg steps. The results are given in Fig. 2. The SAW strain measurements are in good agreement with the strain gauge when the temperature is held constant and the load is increasing. For the second experiment the load was decreased from 1.0 kg to 0 kg in 0.1 kg steps, at room temperature. The results are given in Fig. 3.

For both experiments the SAW sensor data is comparable to the strain gauge data. The SAW sensor data from the two experiments agree very closely with each other as well. The average fractional frequency values versus the average strain values for both increasing and decreasing loads from (Fig. 2 and 3) was plotted in Fig. 4.

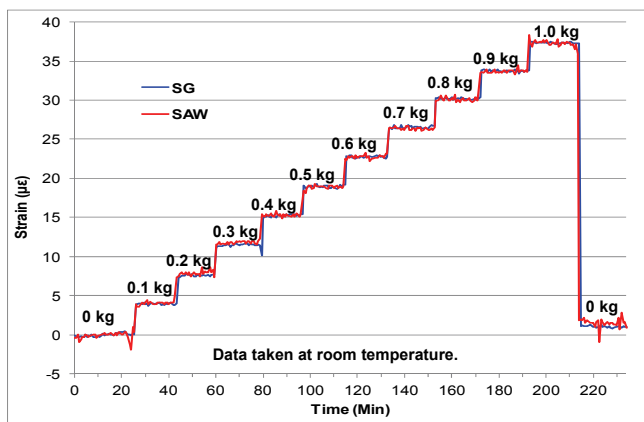


Fig. 2. SAW strain sensor versus strain gauge data at room temperature.

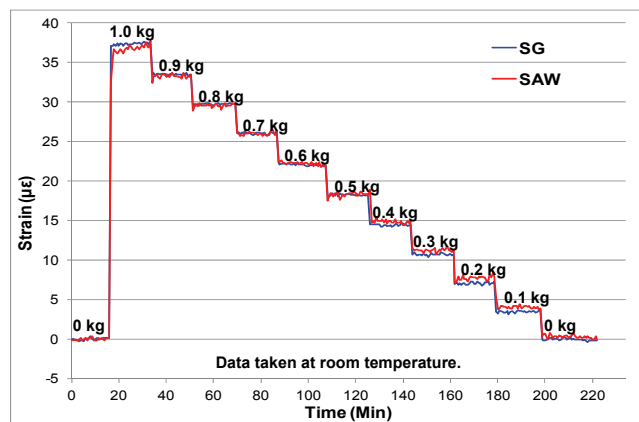


Fig. 3. SAW strain sensor versus strain gauge data at room temperature.

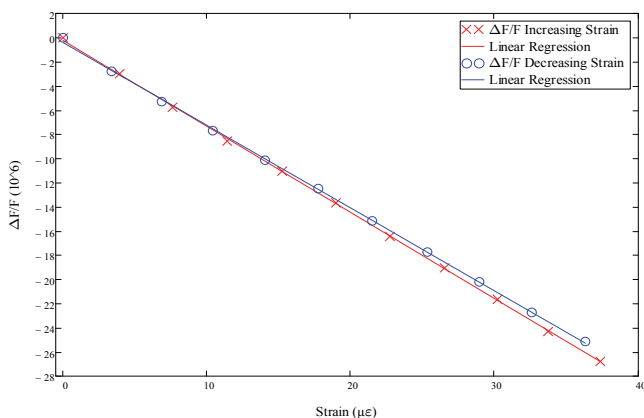


Fig. 4. The average fractional frequency values versus the average strain values for both increasing and decreasing loads shown in Fig. 2 and Fig. 3.

The lines in Fig. 4 are calculated using linear regression. The slopes agree closely, -0.696 for the increasing strain and -0.666 for the decreasing strain data. The small offset in the lines is probably due to small temperature difference (on the order of a few degrees) between the experiments which occurred on different days. Using Eqn. 4 the strain coefficient (γ_s) was calculated to be -0.304 for increasing strain, and -0.334 for the decreasing strain case. The average of the two numbers ($\gamma_s = -0.319$) is used for subsequent calculations. The strain coefficient will be different for different crystal cuts and orientations of the SAW device on the wafer. These values are for a Langasite crystal with an Euler orientation of $(0, 138.5, 26.6)$ with propagation in the X direction.

To characterize the SAW sensor for temperature effects the bar was unloaded and the temperature was raised quickly using a heat gun to a peak of 29.8°C . The bar was then allowed to cool slowly while data was recorded (Fig. 5). The frequency shift data from the SAW device was converted to temperature using $1.6667^\circ\text{C}/\text{Hz}$ (green line). The SAW data agrees closely with the thermocouple (blue line) and is within $\pm 0.28^\circ\text{C}$.

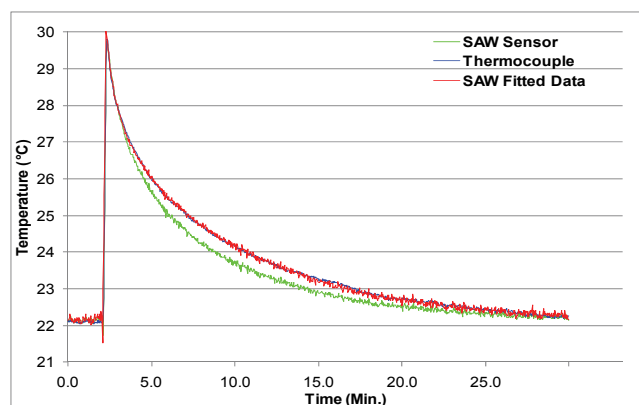


Fig. 5. SAW data, thermocouple data, and SAW values fitted to the thermocouple.

The differences between the SAW sensor and the thermocouple are in part due to the thermal characteristics of the Langasite material and the adhesive between the sensor and stainless steel bar. To adjust for these differences a 3rd order polynomial regression (red line) was used to fit the SAW values to those of the thermocouple:

$$y = 0.0118x^3 - 0.9400x^2 + 25.7931x - 216.0195. \quad (12)$$

The SAW sensor data and (Eqn. 12) can be used as a temperature sensor as long as the device is unloaded and is not experiencing any strain changes.

The temperature coefficient of velocity (γ_T) was calculated to be -0.323 , using Eqn. 8 and 10 along with the SAW data. This coefficient will be used to temperature compensate the SAW strain values.

To characterize the combined strain and temperature measurement capabilities, the cantilevered test specimen was subjected to mechanical strain (tension) from a 0.500 kg mass at room temperature (nominally $21.46^\circ\text{C} \pm 0.15^\circ\text{C}$). The mass was removed after ~ 15 minutes, leaving the bar unloaded at room temperature.

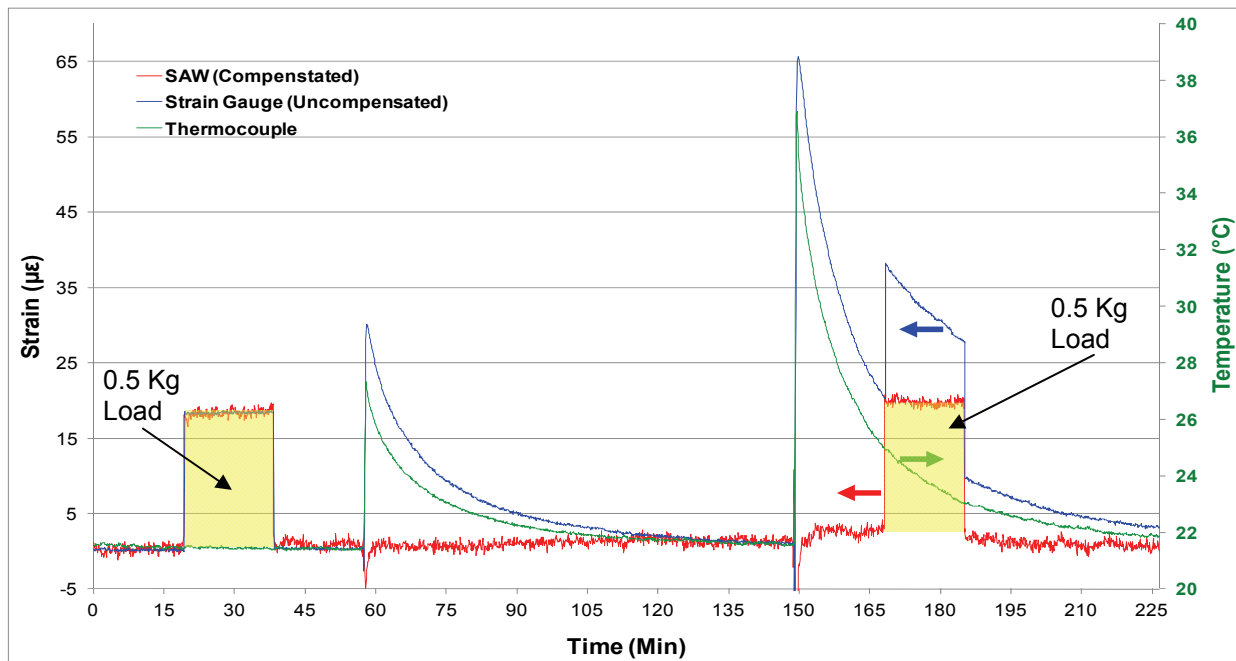


Fig. 6. Temperature compensated SAW sensor data versus strain gauge and thermocouple data.

Next the temperature of the bar was raised quickly to 27.3°C, and allowed to cool to close to room temperature. Then the bar temperature was raised to 36.89°C and the bar was again allowed to cool. Before the bar cooled to room temperature a 0.500 kg mass was placed on the bar and was removed after ~15 minutes while the bar was cooling. The bar was allowed to cool unloaded for an additional 40 minutes. The results from the strain gauge, the thermocouple, and the temperature compensated SAW sensor are given in Fig. 6. The compensation method uses both the strain coefficient of velocity and the temperature coefficient of velocity to remove temperature effects from the SAW data. The compensation technique is effective; however, the large temperature differences still cause small perturbations in the compensated data that need to be eliminated.

5 CONCLUSIONS

The strain (-0.319) and temperature (-0.323) coefficients of velocity have been presented. The coefficients have been demonstrated to be effective at temperature compensating the strain measurements. The initial application of heat creates artifacts; therefore, more work is needed to optimize the technique to provide more accurate results. Further characterization of the sensors will make them more applicable to aerospace applications such as NASA's Vehicle Safety Systems Technology program.

REFERENCES

[1] J. Tikka, *et al.*, "Strain Gauge Capabilities in Crack Detection," presented at the Fourth International

- Workshop on Structural Health Monitoring, Stanford, CA, Sept. 15-17, 2003.
- [2] W. C. Wilson, *et al.*, "Passive Wireless SAW Sensors for IVHM," in *Frequency Control Symposium, IEEE International*, May 19-21, 2008, pp. 273-277.
- [3] A. L. Nalamwar and M. Epstein, "Surface Acoustic Waves in Strained Media," *Journal of Applied Physics*, vol. 47, pp. 43-48, 1976.
- [4] H. Takeuchi and H. Yamauchi, "Strain Effects on Surface Acoustic Wave Velocities in Modified PbTiO₃ Ceramics," *Journal of Applied Physics*, vol. 52, pp. 6147-6150, 1981.
- [5] M. B. Schulz, *et al.*, "Temperature Dependence of Surface Acoustic Wave Velocity on α Quartz," *Journal of Applied Physics*, vol. 41, pp. 2755-2765, 1970.
- [6] Y. Nakagawa, "Control of Second Order Temperature Coefficient of SAW Propagating in Two Thin Film Layers," in *Ultrasonics Symposium, 1993. Proceedings, IEEE*, Baltimore, MD, Oct. 31 - Nov. 3, 1993, pp. 287-290.
- [7] D. C. Malocha, *et al.*, "Measurements of LGS, LGN, and LGT Thermal Coefficients of Expansion and Density," *Ultrasonics, Ferroelectrics and Frequency Control, IEEE Transactions on*, vol. 49, pp. 350-355, 2002.
- [8] W. Wilson, *et al.*, "Fastener Failure Detection using a Surface Acoustic Wave Strain Sensor," *Sensors Journal, IEEE*, vol. PP, p. 9, Dec. 22 2011.
- [9] K. Hashimoto, *Surface Acoustic Wave Devices in Telecommunications: Modelling and Simulation*. Berlin: Springer, 2000.